Cement and Concrete Research 41 (2011) 1123–1129

Contents lists available at ScienceDirect

Cement and Concrete Research

journal homepage: http://ees.elsevier.com/CEMCON/default.asp

The hydration of reactive cement-in-polymer dispersions studied by nuclear magnetic resonance

A.M. Olaru [a], O. Weichold [b,1], A. Adams [a,*]

[a] Institut für Technische und Makromolekulare Chemie, RWTH Aachen University, Templergraben 55, 52056 Aachen, Germany
[b] DWI an der RWTH Aachen, e. V., Pauwelsstraße 8, 52056 Aachen, Germany

ARTICLE INFO

Article history:
Received 4 March 2011
Accepted 30 June 2011

Keywords:
Hydration (A)
Dispersion (A)
Polymers (D)
Characterization (B)
NMR

ABSTRACT

The behaviour of two novel cement-in-polymer (c/p) dispersions, namely cement-in-poly(vinyl acetate) and cement-in-poly(vinyl alcohol) upon exposure to water at room temperature was investigated by a combination of various NMR methods. The swelling, cracking, and the water ingress were monitored non-destructively using ^{1}H single point imaging. The hydration of the cement matrix was investigated using ^{29}Si NMR whilst ^{13}C CPMAS NMR spectra allowed the quantification of the kinetics of the hydrolysis reaction of poly(vinyl acetate) into poly (vinyl alcohol). The polymer controls the rate of water ingress and swelling which in turn determines the behaviour of the c/p dispersions upon exposure to water. For the cement-in-poly(vinyl alcohol), the rates of water ingress and swelling are much faster than the hydration of the clinker whilst for the cement-in-poly(vinyl acetate) the slow rates of the two processes allow the formation of a cementious matrix which assures the stability of the sample.

1. Introduction

Within the last decade, the research interest in textile-reinforced concrete has increased significantly [1,2]. This is mainly due to the fact that this material allows the construction of thin concrete elements, which are unavailable with conventional steel reinforcements. Thin concrete elements are the key to a novel type of architecture that combines the elegance of wood and steel constructions with the material properties of reinforced concrete [3]. More importantly, thin textile-reinforced concrete elements require less cement for their preparation and as a direct result lead to a significant reduction of the CO_2 emission.

For price and strength reasons, glass is the material of choice to prepare the textile reinforcement. Due to the brittleness of glass, the textile is made from glass rovings, i.e. a multifilament yarn consisting of approx. 1600 individual filaments of 10–30 μm in diameter [4,5]. The performance of rovings as reinforcements largely depends on how well the roving is penetrated by the concrete [4,6]. To spark the formation of a cementitious matrix inside the roving, a cement-in-polymer dispersion – abbreviated as c/p in analogy to water-in-oil emulsions – was developed that consists of non-hydrated cement (clinker) dispersed in a water or alkali-soluble polymer. This dispersion is coated onto the roving in such a way that it fills the voids between the individual filaments before it is embedded in concrete [7,8]. Rovings coated with such dispersions exhibit significantly increased pull-out loads and work. Scanning Electron Microscopy (SEM) investigations revealed the formation of crystalline material inside and around the roving. However, differences in terms of mechanical performance and microstructure were observed when comparing dispersions based on poly(vinyl acetate) with those based on poly(vinyl alcohol) [8]. SEM and mechanical analyses provide only information about the final situation of the system, i.e. after hardening and testing, so that mechanistic conclusion concerning the reactivity and behaviour of the dispersions remains to some extent hypothetical. In contrast, methods that provide detailed and real-time insight into how both components of the coating, namely polymer and clinker, interact with the incoming water should allow the elaboration of the mechanistic details. Such data is a basis for explaining the observed differences in the mechanical performance and the morphology of the interface of the two coatings and is a requirement to tune future dispersions for specific applications using other reactive inorganic additives.

Compared with SEM and mechanical testing, Nuclear Magnetic Resonance (NMR) is particularly favourable for the investigation of cement-based materials as it is fully compatible with water-wet samples and allows analysing the bulk of opaque sample in a truly non-destructive fashion [9–11]. ^{1}H relaxation, imaging, and self-diffusion NMR were successfully applied to investigate the water ingress, drying, and moisture distribution in ordinary Portland cement and to evaluate the effect of various additives [9–19]. Specifically, magnetic resonance imaging (MRI) provides a unique way to monitor non-destructively and with submillimetre resolution the ingress of

* Corresponding author. Tel.: +49 241 8026428; fax: +49 241 8022185.
E-mail address: aadams@mc.rwth-aachen.de (A. Adams).
[1] Present address: Institute of Building Materials Research, RWTH Aachen University, Schinkelstr. 3, 52062 Aachen.

0008-8846/$ – see front matter © 2011 Elsevier Ltd. All rights reserved.
doi:10.1016/j.cemconres.2011.06.015

water in a continuous way in cementious materials. However, classical MRI of cement materials is extremely challenging due to short spin–spin (T_2) relaxation times that the water exhibits inside these materials and also due to local magnetic inhomogeneities which raise technical difficulties in acquiring the image and considerably depreciate its quality [20]. These problems can be avoided by using Single Point Imaging (SPI) [11–14], a pure phase encoding technique which has the important advantage of being free of susceptibility artefacts, an essential feature for accurate high resolution imaging of nuclei with short spin–spin relaxation [18].

^{29}Si NMR spectroscopy has been shown to be a very useful technique to characterise in detail the reaction of water with calcium silicate phases, which are the major components of ordinary Portland cement [21–25]. The individual SiO_4 tetrahedron of the anhydrous clinker phases is transformed due to hydration into the C–S–H gel, through silicate polymerization. As the C–S–H is quasi-amorphous very few experimental techniques are available for its detection and characterization. Amongst them NMR is very often the method of choice as it can provide local structural information even in the absence of long-range structural order. The ^{29}Si NMR chemical shifts of silicates range between −60 and −140 ppm and allow the characterization of the various tetrahedral Qn environments as each Q site gives a NMR signal at a distinct chemical shift [26].

Herein we present a nuclear magnetic resonance (NMR) study on two exemplar coatings, namely cement-in-poly(vinyl alcohol), abbreviated as c/PVA, and cement-in-poly(vinyl acetate), abbreviated as (c/PVAc). Besides the protons of water, the c/p dispersions contain carbon and silicon as NMR-active nuclei so that a combination of NMR methods provides the means to gather information on all relevant components. By using a combination of 3D ^{1}H NMR SPI, ^{29}Si NMR, and ^{13}C cross-polarisation under magic angle spinning (CPMAS), the water ingress, the reaction of the cement clinker, and polymer hydrolysis can be studied non-invasively as a function of time. This unique set of data allows the elaboration of mechanistic details and the explanation of the different behaviour of the two samples.

2. Experimental section

2.1. Materials

Poly(vinyl alcohol), PVA, M_w = 9500, saponification number 302, and poly(vinyl acetate), PVAc, M_w = 110,000–150,000, were obtained from Wacker Chemie AG, Burghausen, Germany. The chemical structures of the two polymers are shown in Fig. 1. A fine-grained Portland cement with a particle size $d_{95} \leq 6$ μm was obtained from Dyckerhoff AG, Neuwied, Germany.

2.2. Sample preparation

In a typical preparation, 210 g cement and 90 g of polymer are used resulting in a 70/30 mixture by weight. In the case of PVA, the polymer is plasticised in a Brabender Plastograph® at 150 °C, whilst in the case of PVAc, the polymer and 5 ml of *n*-butyl acetate are placed in an IKA HKD-T 0.6 laboratory kneader, warmed up to 65 °C, and kneaded until the mixture is soft and appears homogeneous. Then the cement is slowly added in ten portions. After the final cement portion is added, agitation is continued for approx. 10 min. The warm mixture is poured onto a Teflon plate and allowed to cool in a fume hood. When completely solidified, the mass is broken into pieces of approx. 1 mm in size, melted at 150 °C, and extruded through a round die into 4 mm thick strands.

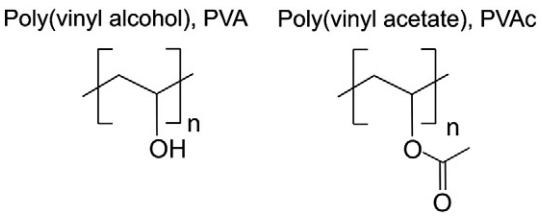

Fig. 1. Chemical structures of poly(vinyl alcohol), PVA, and poly(vinyl acetate), PVAc, used to prepare the c/p dispersions under investigation.

2.3. ^{1}H NMR imaging experiments

The proton NMR imaging experiments have been performed at room temperature using a 200 MHz Bruker DSX spectrometer with a 10 mm birdcage resonator. The cylindrical samples have been immobilised inside standard glass tubes (Fig. 2), with an inner diameter of 9 mm, in such a way that the water ingresses into the sample only from the long sides and in order to ensure that no movement artefacts due to the gradient ringing affect the image quality. The samples were continuously kept in water up to 96 h and the images were acquired using a standard 3D single point imaging (SPI) NMR sequence [27,28]. The use of 3D SPI gives the true picture of the water ingress, provides detailed information about the homogeneity of the samples, and allows a much better visualisation of the formation of the cracks.

The 3D SPI images with a digital resolution of 78 × 78 × 780 μm were obtained by using a pulse length of 3 μs, a phase encoding time t_p of 41 μs and a maximum gradient strength of 0.93 T/m. A repetition time of 50 ms allowed the suppression of the free water signal outside the sample and ensured high contrast in the images. The chemical bound water inside the samples has a T_2*shorter than the encoding time and therefore it has no contribution to the detected signal [11]. Although a complete elimination of the spin–spin relaxation time weighting of the images is virtually impossible, the proper choice of the acquisition parameters and the correction of the image intensities as a function of the local effective spin–spin relaxation time can provide true spin-density maps of the water inside the sample [11]. However, care should be taken for quantitative comparison of the local signal intensities in the images of the two samples at different exposure times. Despite the high gradient amplitudes which were employed for the experiments, the short encoding time used ensures that the signal loss due to the molecular diffusion caused by the gradients is negligible. The imaging data have been evaluated by using Prospa (Magritek Limited, Wellington, NZ).

2.4. ^{13}C and ^{29}Si NMR experiments

^{13}C and ^{29}Si high-resolution spectra were recorded with a Bruker DSX500 NMR instrument working at frequencies of 500.12 MHz for protons, of 125.44 MHz for ^{13}C, and of 99.43 MHz for ^{29}Si. All measurements were performed at room temperature using a 4 mm probe under magic angle spinning (MAS) conditions at a spinning

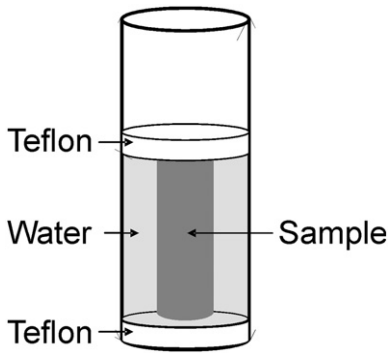

Fig. 2. Schematic illustration of the experimental setup together with the aspect ratio of the relative geometries used to monitor the water ingress into the extruded, cylindrical samples.

speed of 5 kHz. Some of the measurements were later on verified using an AV700 NMR Bruker spectrometer.

High-resolution ^{13}C MAS spectra were obtained using the cross-polarisation method with a contact time of 1 ms and a recycle delay of 5 s. The spectra were calibrated to the chemical shifts of adamantane.

For the ^{29}Si MAS NMR single-pulse experiments were recorded using proton decoupling during acquisition. As the samples are prepared from ordinary Portland cement, they contain Fe^{3+} in the form of calcium aluminate ferrite ($C_4AF = 4\ CaO \cdot Al_2O_3 \cdot Fe_2O_3$) as paramagnetic impurity. This leads to a decrease in the spin–lattice relaxation time and, consequently, allows a substantial reduction of the repetition time needed to record quantitative ^{29}Si spectra. It was found that a repetition time of 10 s is enough to obtain quantitative data. This allowed to monitor the progress of the hydration of the cement by recording the spectra of samples exposed to water for different periods of time. The ^{29}Si chemical shifts are referenced to the chemical shifts of SiO_2. The ^{29}Si isotropic chemical shift of the peaks were analysed using the Q_n classification: Q_0 represents monosilicates, whilst Q_1 represents disilicates and chain end groups, Q_2 middle groups in chains, Q_3 chain branching sites, and Q_4 three-dimensional cross-linked framework [26]. The obtained spectra were analysed with the help of the DMFIT program [29] by using Lorentzian functions.

In order to follow the hydrolysis of PVAc to PVA and to get information about the hydration process of the cementious matrix, the various c/p samples were stored into water for different times and then removed in order to stop the ingress process. A piece of small length was then cut out from the cylindrical sample through the whole transverse section and grinded to a fine powder for filling the MAS rotor.

3. Results

3.1. Swelling, cracking, and water ingress monitored by ^1H NMR imaging

The water inside cement-based materials exhibits not only short T_2 relaxation times (approx. 0.3–1 ms, depending on the pore-size distribution and on the exposure times) but also short spin–lattice T_1 relaxation times. As the T_1 values of the free water outside the sample and of the polymer are in the order of seconds (measured by the inversion-recovery method), these signals can be suppressed by using a proper repetition time, which is in the present case 50 ms. In consequence, only the signal from water molecules inside the sample will be detected. This allows the continuous monitoring of the water ingress into the sample.

The position of the water front inside the two samples at different exposure times is depicted in Figs. 3 and 4. The front of water ingress is represented by the bright colours (the brighter the colour the higher the signal intensity) whilst the black colour represents regions of the sample containing no water. For reasons of clarity, only 2D slices extracted from the recorded 3D images are depicted. They correspond to the middle of the samples. The other slices show similar behaviour.

The images reveal a completely different behaviour of the two samples in contact with water. The water ingress into the c/PVA sample is very fast (Fig. 3). Swelling is very pronounced and the volume increase is only restricted by the dimensions of the glass tube containing the sample. At exposure times greater than about 4 h, macroscopic cracks start to develop and a fractal-like surface is generated. This facilitates an even faster water uptake which ultimately leads to massive cracking of the sample before the water front reaches the centre of the sample (approximately 6 h).

In contrast, water ingress into the c/PVAc sample is very slow and it takes about 3 days until the sample is fully saturated (Fig. 4). Moreover, during this time the sample develops almost no cracks and

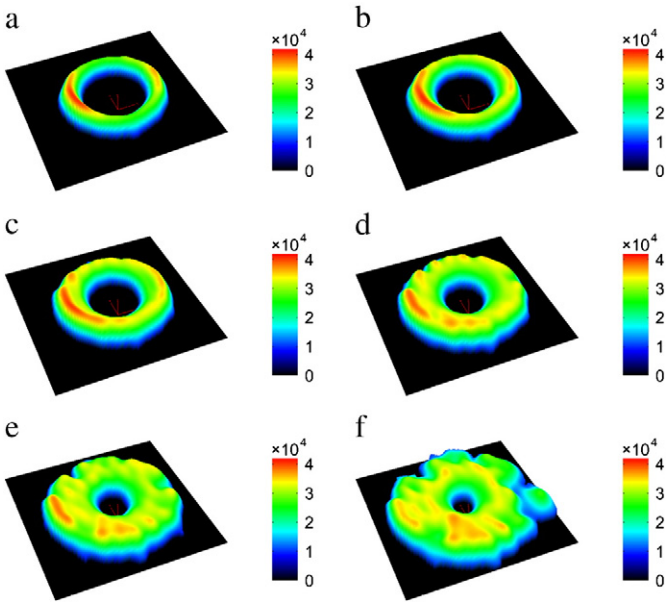

Fig. 3. Images of a c/PVA sample acquired after (a) 15 min, (b) 30 min, (c) 1 h, (d) 2 h, (e) 3 h, and (f) 4 h of exposure to water. The water reaches the middle of the sample in about 6 h.

the changes in shape are minimal. For longer exposure times the sample reaches a steady-state (Fig. 4e, f).

To study the differences between the samples in greater detail, the changes in the outer radius of both samples with exposure time were measured using data extracted from the images (Fig. 5). This allows a quantification of the swelling behaviour of the two samples. As the initial radii of the samples were not identical, they were measured manually before exposure to water. In the case of the c/PVA sample, the radius was measured up to the point where the sample cracks, whilst for the c/PVAc sample, the measurements were continued until the radius reached a constant value.

During the first 6 h in contact with water, the c/PVA sample shows an increase in radius of about 70% whilst the radius of the c/PVAc is nearly not changing. The latter reaches its steady-state of about 15%

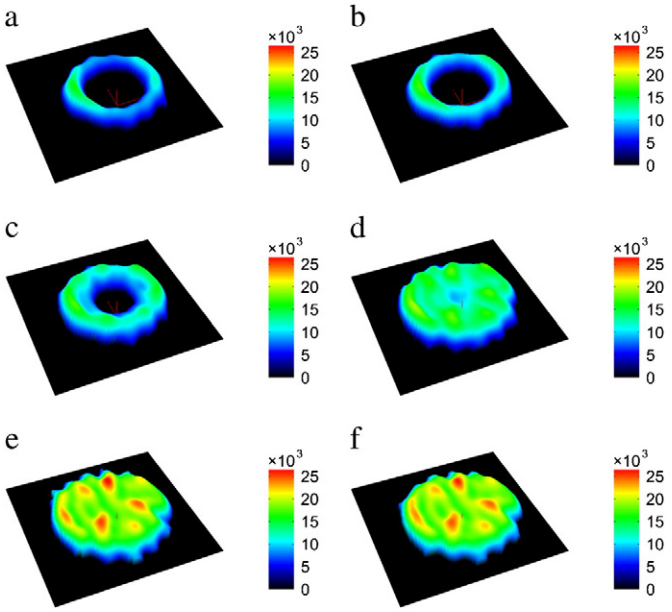

Fig. 4. Images of a c/PVAc sample acquired after (a) 8 h, (b) 12 h, (c) 24 h, (d) 48 h, (e) 72 h, and (f) 96 h of exposure to water.

within 48 h. It was also observed that the increase in radius of the c/PVA at times higher than 1 h is approximately linear with a rate of about 0.22 mm·h^{-1}. In contrast, the increase in radius of the c/PVAc exhibits three regimes (Fig. 5). The first two regimes are roughly linear with the exposure time whilst the third regime is a steady-state. In the regime I, which corresponds to the first 12–14 h, the increase in the radius is extremely slowly, being described by a rate of about 0.002 mm·h^{-1} whilst at higher exposure times (regime II) the increase in the radius is about five times faster, being characterised by a rate of 0.01 mm·h^{-1}. The estimated rates are also strongly indicating the completely different swelling behaviour of the two c/p samples.

Another parameter used to quantify the changes in the samples induced by the water ingress is the crack ratio which we defined as the ratio of the length of the circumference including the cracks to the length of the circumference without cracks. For that, the NMR images have been converted into a binary representation (Fig. 6a). As this representation depends on the achieved resolution the estimated crack ratio may be different for different resolutions. However, for the same resolution, the crack ratio represents a useful parameter to follow the cracking behaviour of the two samples under investigation.

The evolution of the cracking phenomenon has an exponential form for both samples. This process is characterised by a rate of 0.55 h^{-1} for c/PVA whilst for c/PVAc the rate is of 0.01 h^{-1} which means that the cracking process is about 55 times slower than for c/PVA (Fig. 6b). Moreover, the cracking process for this last sample stops once the sample is fully hydrated, most probably due to the hardening of the cement which is accompanied by the formation of a strong matrix.

Since the advancement of the water front could be observed directly, its real-time evaluation can be used to obtain information about the rate of water ingress. The advancement can be represented in two ways: (1) by the distance of the surface of the swollen sample to the advancing front (directly measured on the images) and (2) by the diffusion distance d determined by the following formula:

$$d = \tfrac{1}{2}\,(d_0 - c) \tag{1}$$

where d_0 is the original sample diameter and c is the diameter of the remaining "dry" core measured on the images. In this way, the diffusion processes alone can be evaluated by correcting it for the swelling of the sample.

The variation of the diffusion distances with the exposure time is depicted in Fig. 7. For both samples a linear dependence is observed for the whole exposure interval which allowed the estimation of the rate of water penetration. In the case of the c/PVA the rate is 0.22 mm·h-1 whilst for the c/PVAc the rate is 0.035 mm·h^{-1}.

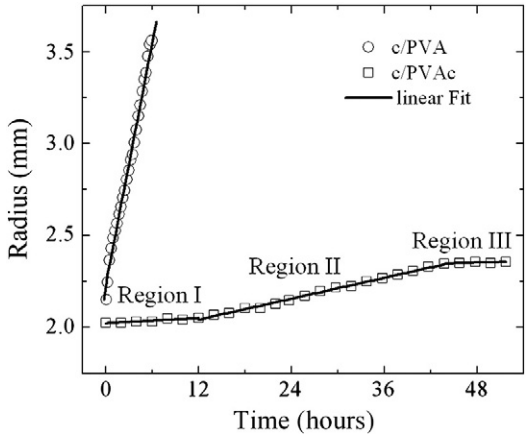

Fig. 5. The swelling of c/PVA and c/PVAc upon exposure to water reflected in the changes of the radius.

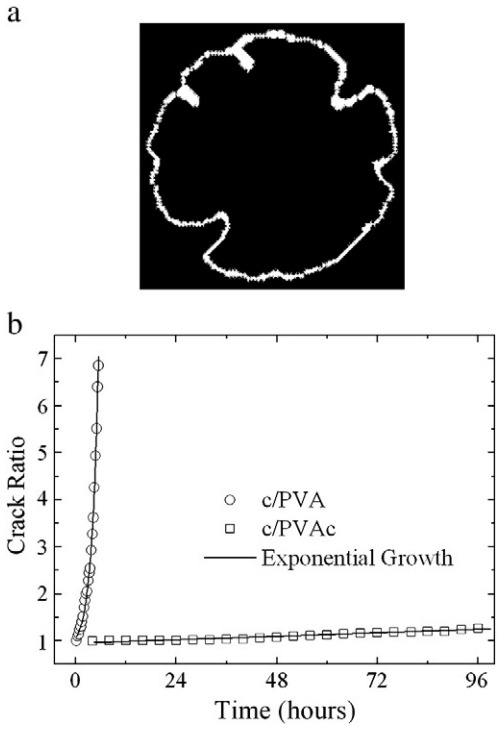

Fig. 6. (a) Example of an image converted to binary form. (b) The crack ratio as a function of the time the sample has been exposed to water and the corresponding fit using the fitting function $y = y_0 + A e^{kt}$ where y_0 was set to 1 for both samples and k is the constant rate.

3.2. Hydration of the cementious matrix by ^{29}Si NMR

The ^{29}Si spectra of the c/p samples obtained in single-pulse experiments with proton decoupling during acquisition are depicted in Fig. 8a. The anhydrous c/PVAc and c/PVA samples show only Q_0 groups and a broad resonance located at approximately −110 ppm due to the Q_4 groups belonging to the quartz in the cement. During exposure to water, additional signals of Q_1 and Q_2 groups appear in the ^{29}Si NMR spectrum as observed in Fig. 8a for the c/PVAc sample. The ^{29}Si NMR spectra of the c/PVA show similar behaviour. No signals from Q_3 or Q_4 groups other than those belonging to quartz were detected, in agreement with other ^{29}Si NMR studies on cement materials [22,30]. With increasing the exposure time, the intensity of the Q_0 signal is reduced and the intensities of the Q_1 and Q_2 signals become stronger. This is a clear indication that the water reacts with the clinker to form C–S–H phases.

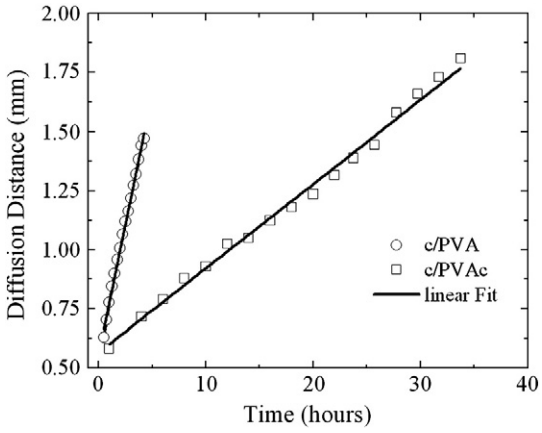

Fig. 7. Variation of the diffusion distance d with the exposure time to water.

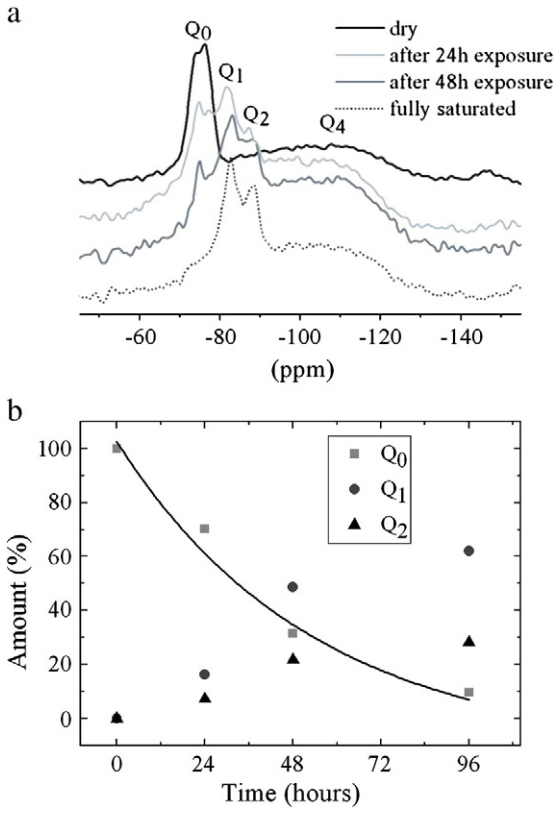

Fig. 8. (a) ^{29}Si NMR spectra of c/PVAc samples before and after exposure to water. (b) Relative amounts of the silicate species present during the reaction of c/PVAc with water. The data was extracted from ^{29}Si NMR spectra with the help of a line-shape simulation. The line represents the fit with an exponential decay corresponding to a first-order reaction.

The analysis of the quantitative ^{29}Si spectra confirmed the initial qualitative finding that Q_1 and Q_2 species are formed at the expense of anhydrous clinker phases as the exposure time increases. The amount of both Q_1 and Q_2 species increased with the exposure time, a process which is faster for the Q_1 groups than for the Q_2 (Fig. 8b). In the case of the c/PVAc sample, after 24 h of exposure, approx. 70% of the clinker still exists in the anhydrous phase whilst after 48 h of exposure (when the sample is almost fully saturated) about 30% of the clinker appears not to have reacted. Moreover, Q_0 groups are still present even after the sample is saturated with water. This is consistent with previous SEM investigations [8]. The reaction of water with the cement clinker follows a first order law with a constant rate of approximately 0.02 h^{-1}.

In the case of c/PVA, the corresponding ^{29}Si NMR spectrum after 4 h in water, when the sample is almost fully saturated, shows no changes compared to the spectrum of a non-hydrated sample. Only after exposure times much longer than the time needed for the water to reach the middle of the sample, signals belonging to Q_1 and Q_2 groups appear in the spectrum. As an example, after 24 h of exposure, about 75% of the clinker is still in the anhydrous phase whilst after about 48 h of exposure, about 33% of the clinker did not react. The obtained values indicate that the decrease of the clinker takes place at nearly the same rate like in c/PVAc.

3.3. Kinetics of the hydrolysis of PVAc into PVA by ^{13}C CPMAS NMR

As pure PVAc deacetylates into PVA in the presence of an alkali medium, ^{13}C CPMAS was employed to find out if this reaction takes place also for the polymer inside the c/PVAc and at what rate. The resonance assignment of the c/PVA and c/PVAc was done based on the signal assignment of the pure polymers according to Ref. [31]. Pure PVAc shows signals around 21 ppm (methyl group), around 40 ppm (methylene group), around 67 ppm (methine group), and around 170 ppm (carboxyl group). Pure PVA shows a peak at around 44 ppm (methylene groups) and three peaks at about 65 ppm, 70.5 ppm and 76 ppm (methine groups). The splitting of the methine signal is related to the number of intermolecular hydrogen bonds with the neighbouring hydroxyl [32].

In order to optimise the response of the ^{13}C CPMAS spectra and to ascertain the parameters necessary for a quantitative assessment, several contact times were tested for the c/p samples. For a contact time of 1 ms, a good agreement of the CP spectra with those obtained using direct polarisation experiments recorded with recycle delay times of 400 s for quantitative results was found, in agreement with other studies [33]. Additionally, ^{13}C T_1 NMR measurements performed using the Torchia method [34] for the two c/p samples showed the existence of a short relaxation time in the range of seconds and of a long relaxation time in the range of tens of seconds (up to 60 s) for most signals of the two polymers. The short component can be attributes to an amorphous phase whilst the long one to a crystalline phase [33,35]. This is a clear evidence that both polymers in the two c/p dispersions are semicrystalline [32,33]. Moreover, the effect of the paramagnetic impurities existing in the clinker on the relaxation times of the polymer are negligible because the estimated relaxation times are in the same range like those reported by other groups for the pure polymers [32,33,35].

The ^{13}C CPMAS spectra of c/PVAc before and after exposure to water are shown in Fig. 9a. In the spectrum of the dry c/PVAc sample both methylene and carboxyl group give rise to a single peak whilst the spectrum obtained after 96 h in water resembles that of pure PVA.

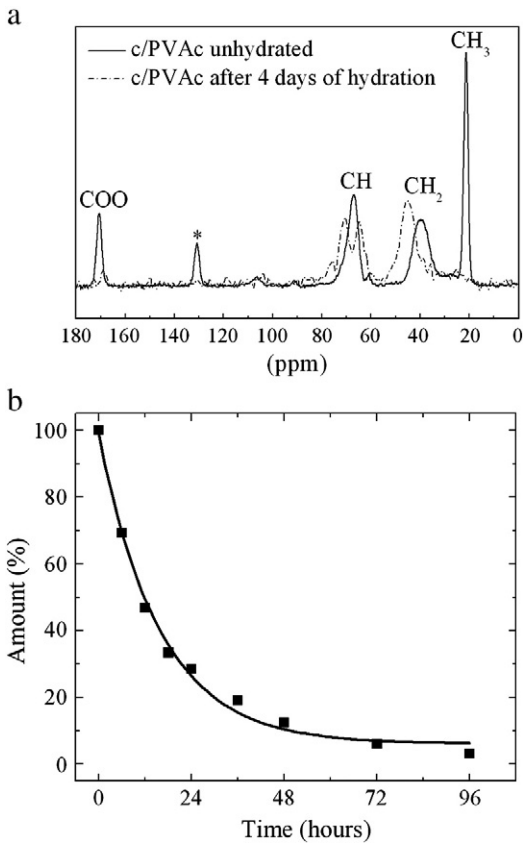

Fig. 9. (a) ^{13}C CPMAS NMR spectra of c/PVAc before and after 4 days of exposure to water. The signal marked with a star represents a spinning sideband. (b) Extent of hydrolysis of PVAc as a function of the exposure time to water. The line respresents the fit corresponding to a first-order reaction.

Additionally, a small peak at around 25 ppm is found, which was assigned to calcium acetate [33]. Both results confirm that PVAc was hydrolysed to PVA. The peak at about 168 ppm was assigned to calcium carbonate formed by trapping residual CO_2 from the atmosphere [33].

The kinetics of the hydrolysis reaction, as monitored with the help of CPMAS spectra, is depicted in Fig. 9b. During the first 12 h of exposure to water, approx. 50% of the acetate groups are hydrolysed, whilst after 48 h, when the sample is almost fully saturated, approx. 10% of the acetate groups are still left. The hydrolysis of the acetate groups follows a first-order kinetic with a constant rate of about 0.1 h^{-1}.

4. Discussion

The combination of various NMR methods employed during this study raises the possibility to independently study the interaction of each component of the dispersions, namely the polymer phase and the clinker, with the incoming water. As ^{29}Si NMR gave insights into the hydration of the clinker and the ^{13}C CPMAS follows the hydrolysis of the polymer phase, ^{1}H SPI NMR allows to online monitor how the changes experienced by the two components of the dispersions are affecting the swelling, diffusion, and cracking of the samples. In such a way, an understanding of the complex interplay of the various factors which are responsible for the differences in the final mechanical stability of the two samples are gained.

The SPI images show that the two samples have completely different behaviour upon exposure to water. For the c/PVA the water ingress is very fast and the swelling is very pronounced. Until the sample cracks both processes evolve at the same rate of 0.22 mm·h^{-1}. Afterwards, large cracks develop which facilitate even more water uptake and the sample is fully saturated in about 6 h. During this time, the clinker has not reacted with the incoming water, as observed from ^{29}Si NMR, this being an essential step for the formation of a cementious matrix. In the absence of this matrix, the sample starts to crack due to the strong swelling of the polymer matrix. If amorphous PVA simply dissolves by contact with water, the amount of crystallinity is controlling not only the speed of the water ingress but also the extent of swelling for semicrystalline PVA [36,37]. Studies showed that the dissolution of the crystals upon exposure to water is a complex process which takes place only if enough water is available [36]. The crystals are not swelling by contact with water but they will gradually be destroyed as the water molecules attack the crystallites at the crystalline/amorphous interface [37,38]. In this way the amount of the amorphous phase increases and in consequence the amount of water in the polymer which will lead to further swelling [37]. The time required for complete dissolution strongly depends on the amount of crystallinity and the dissolution conditions [37]. Additional ^{13}C NMR measurements performed on c/PVA show that an extremely low amount of polymer still exists in the sample after prolonged exposure to water which is an indication that the polymer dissolves.

In contrast, c/PVAc shows a completely different behaviour. The water ingress is slow, and the swelling and cracking are rather limited. The sample preserves its shape upon longer exposure time this being an indication of higher mechanical stability than that of c/PVA.

In contact with water, three stages can be identified for c/PVAc based on the changes in its outer radius. In the first stage, during the first 12–14 h of exposure to water, the swelling of the sample is rather limited being characterised by a rate of 0.002 mm·h^{-1}whilst in the second stage (until about 48 h) the swelling is getting about 50 times stronger being characterised by a rate of 0.01 mm·h^{-1}. In both cases the swelling is at least with an order of magnitude lower than for the c/PVA. During both stages the rate of ingress of water is 0.035 mm·h^{-1} and is higher than the swelling rate. The rate of water ingress for c/PVA is about one order of magnitude lower compared with the rate for c/PVAc. The third stage (after 48 h) is steady-state: the sample is fully saturated with water and no changes in its shape can be further observed.

The behaviour described above can be related to the fact that PVAc is insoluble in water but hydrolyses to form PVA in the presence of alkali. This reaction could be confirmed and its extent could be monitored with the help of ^{13}C CPMAS experiments. The kinetics of the hydrolysis follows a first-order reaction with a rate of 0.1 h^{-1}. At the beginning of the exposure of the sample to water, traces of water absorbed by PVAc will react with the clinker, which liberates alkali in the form of $Ca(OH)_2$ and, to a lower extent, NaOH. The consequential increase of the pH promotes the hydrolysis of PVAc to PVA. As the water is not penetrating the crystalline regions, the hydrolysis should take first place in the amorphous regions and then gradually in the crystalline regions by the hydrolysis of the acetate groups at the crystalline/amorphous interface. Up to 12 h, around 50% of the acetate groups are hydrolysed and only after this the c/p sample shows limited swelling. After 48 h, when the sample is almost saturated, about 10% of the acetate groups are still not hydrolysed. This could be related to the existence of acetate groups in crystalline regions which are not exposed to the incoming water. Even after 96 h some acetate groups still exist which may be an indication that the hydrolysis of these groups in the crystalline phase is a fairly slow process. This can be attributed to the hydrophobic nature of PVAc which together with its semicrystalline nature which constraint not only the amount of the water uptake by the amorphous regions but also slow down the water ingress in the dispersions. This, in turn, allows the clinker to have enough time to react with the incoming water. In such a way a cementious matrix forms which restrain the extent of swelling and at longer exposure times assures that no changes in the shape take place. This reaction was confirmed by ^{29}Si NMR which shows the appearance of signals corresponding to the formation of dimers and polymeric chains inside the C–H–S phase. The hydration process of the clinker characterised by a rate of about 0.02 h^{-1} is much slower than the hydrolysis reaction of PVAc into PVA.

The above results clearly show that the mechanical stability of the samples is determined by the interplay between the hydration of the clinker which is the required step for the formation of a cementious matrix and the rates of water ingress and swelling. If the hydration of the clinker, as observed by the ^{29}Si NMR, seems not to be affected by the presence of the polymer, the type of polymer is a key parameter in controlling the behaviour of the two c/p samples upon exposure to water and in consequence their final mechanical stability. The type of polymer determines the rate of water ingress and as well as the degree of swelling of the c/p samples. In the case that the polymer swells very slowly upon exposure to water the clinker has enough time to react with the incoming water and a stable cementious matrix will be formed which assures the stability of the sample. Contrary, if the clinker has not enough time to react with the incoming water the c/p sample will have much less mechanical stability.

As the rate of the various reactions, which take place in c/p upon exposure to water, should be strongly affected by the temperature, the reported results here are, probably, valid only for the behaviour of the p/c samples at room temperature. Therefore, the temperature should be another parameter, next to the polymer type, to control the final stability of the samples. The effect of the temperature may be easy to asses using similar NMR imaging experiments. Work along this line is in progress.

5. Conclusions

In the present study a combination of NMR ^{1}H imaging and ^{13}C and ^{29}Si spectroscopy methods was successfully applied to investigate the behaviour during exposure to water of two novel c/p samples, namely cement-in-poly(vinyl acetate) and cement-in-poly(vinyl alcohol). The use of the ^{1}H SPI imaging technique has allowed a real time, non-invasive monitoring of the water ingress into the dispersions and

has ensured the sensitivity necessary for the observation of the swelling, cracking, and evolution of the front of water ingress. With the help of ^{29}Si NMR the hydration of the cement matrix could be investigated whilst the deacetylation reaction of PVAc into PVA was confirmed and characterised with the help of ^{13}C CPMAS data.

The employed combination of NMR methods clearly indicates that the type of polymer used for the preparation of the p/c samples is the key parameter controlling the behaviour of the dispersions upon exposure to water. The final mechanical stability of the samples is determined by the competition between the rates of swelling, water ingress, and the hydration of the clinker which is the essential step for the formation of a cementious matrix. The type of polymer seems to not affect the rate of the clinker hydration but controls the rate of water ingress and swelling. In case of c/PVA the hydrophilic nature of the polymer favourites the water ingress within a time scale much shorter than the time the clinker needs to be hydrated. As a consequence, the c/PVA sample swells and cracks extensively and it will finally exhibit less mechanical stability. Contrary, for c/PVAc, due to the hydrophobic nature of the polymer, the swelling of the PVAc matrix will only take place when it is deacetylated to a certain degree into PVA. As this reaction is fairly slow, the water ingress into the c/PVAc is taking place at about the same time scale like the hydration of the clinker. In this case a cementious matrix build up which restrict the swelling of the c/PVAc sample and assures its mechanical stability.

To our knowledge, this is the first time that such precise and detailed information about the rate of various reactions in c/p materials are delivered. In such a way, a clear, real-time picture about the parameters responsible for the mechanical stability of the samples was gained.

Moreover, we believe, in a first approximation, that the use of the data only referring to the rate of water ingress and swelling can already give reliable information about the mechanical stability of the samples. Additionally, we are confident that the strategy we are presenting in this paper to characterise the behaviour of c/p samples during exposure to water could be easily extended to other similar materials.

Acknowledgements

This work was supported by Deutsche Forschungsgemeinschaft (SFB 532 — Textilbewehrter Beton). The authors thank Prof. Bernhard Blümich for his support, Franz-Josef Steffens for technical assistance, and the reviewers for their comments.

References

[1] W. Brameshuber, Textile reinforced concrete — state of the art, Report of RILEM Technical Committee 201 (Rilem Report 36), Rilem Publications SARL, Bagneux, France, 2006.
[2] J. Hegger, G. Bertram, T. Dressen, M. Horstmann, T. Roggendorf, Innovative concepts for concrete structure, Beton- Stahlbetonbau 104 (2009) 17.
[3] J. Hegger, H.N. Schneider, A. Sherif, M. Molter, S. Voss, Thin reinforced cement based products and construction systems, A. Dubley, Farmington Hills, 2004, p. 55.
[4] O. Weichold, M. Hojczyk, Size effects in multifilament glass-rovings: the influence of geometrical factors on their performance in textile-reinforced concrete, Text. Res. J. 79 (2009) 1438.
[5] J. Hegger, M. Horstmann, S. Voss, N. Will, Textile reinforced concrete load-bearing behaviour: design and application, Beton- Stahlbetonbau 102 (2007) 362–370.
[6] S. Ohno, D.J. Hannat, Modeling the stress-strain response of continuous fiber reinforced cement composites, ACI Mater. J. 91 (1994) 306.
[7] O. Weichold, M. Möller, A cement-in-poly(vinyl alcohol) dispersion for improved fibre-matrix adhesion in continuous glass-fibre reinforced concrete, Adv. Eng. Mater. 9 (2007) 712.
[8] O. Weichold, Preparation and properties of hybrid cement-in-polymer coatings used for the improvement of fibre-matrix adhesion in textile reinforced concrete, J. Appl. Polym. Sci. 116 (2010) 3303–3309.
[9] N. Nestle, P. Galvosas, J. Kärger, Liquid-phase self-diffusion in hydrating cement pastes — results from NMR studies and perspectives for further research, Cem. Concr. Res. 37 (2007) 398–413.
[10] P.J. McDonald, J. Mitchell, M. Mulheron, Encyclopedia of materials: science and technology, Elsevier, Berlin, 2008.
[11] M. Bogdan, B.J. Balcolm, T.W. Bremner, R.L. Armstrong, Single-point imaging of partially dried, hydrated White Portland cement, J. Magn. Reson. 116 (1995) 266–269.
[12] P.J. Prado, B.J. Balcom, S.D. Beyea, R.L. Armstrong, T.W. Bremner, P.E. Grattan-Bellew, Concrete/mortar water phase transition studied by single-point MRI methods, Magn. Reson. Imaging 16 (1998) 521–523.
[13] S.D. Beyea, B.J. Balcom, T.W. Bremner, P.J. Prado, A.R. Cross, R.L. Armstrong, P.E. Grattan-Bellew, The influence of shrinkage-cracking on the drying behaviour of White Portland cement using Single-Point Imaging (SPI), Solid State NMR 13 (1998) 93–100.
[14] S.D. Beyea, B.J. Balcom, I.V. Mastikhin, T.W. Bremner, A.R. Cross, R.L. Armstrong, P.E. Grattan-Bellew, Imaging of heterogeneous materials with a turbo spin echo Single-Point Imaging technique, J. Magn. Reson. 144 (2000) 255–265.
[15] A.J. Bohris, U. Goerke, P.J. McDonald, M. Mulerhorn, B. Newling, B. Le Page, A broad line NMR and MRI study of water and water transport in portland cement pastes, Magn. Reson. Imaging 16 (1998) 455–461.
[16] P. Faure, S. Caré, C. Po, S. Rodts, An MRI-SPI and NMR relaxation study of drying — hydration coupling effect on microstructure of cement-based materials at early age, Magn. Reson. Imaging 23 (2005) 311–314.
[17] M. Gussoni, F. Greco, F. Bonazzi, A. Vezzoli, D. Botta, G. Dotelli, I.N. Sora, R. Pelosato, L. Zetta, ^{1}H NMR spin–spin relaxation and imaging in porous systems: an application to the morphological study of white portland cement during hydration in the presence of organics, Magn. Reson. Imaging 22 (2004) 877–889.
[18] S.J. Jaffer, C. Lemaire, C.M. Hansson, H. Peemoeller, MRI: a complementary tool for imaging cement pastes, Cem. Concr. Res. 37 (2007) 369–377.
[19] J.J. Young, P. Szomolany, T.W. Bremner, B.J. Balcolm, Magnetic resonance imaging of crack formation in hydrated cement paste materials, Cem. Concr. Res. 34 (2004) 1459–1466.
[20] I.V. Kotyug, R.Z. Sagdeev, Applications of NMR tomography to mass transfer studies, Russ. Chem. Rev. 71 (2002) 789–835.
[21] P. Colombet, A.-R. Grimmer, Application of NMR Spectroscopy to Cement Science, Gordon and Breach, Amsterdam, 1994.
[22] F. Brunet, T. Charpentier, C.N. Chao, H. Peycelon, A. Nonat, Characterization by solid-state NMR and selective dissolution techniques of anhydrous and hydrated CEM V cement pastes, Cem. Concr. Res. 40 (2010) 208–219.
[23] J.J. Beaudoin, L. Raki, R. Alizadeh, A ^{29}Si MAS NMR study of modified C–S–H nanostructures, Cem. Concr. Compos. 31 (2009) 585–590.
[24] E. Lippmaa, M. Mägi, M. Tarmak, W. Wieker, A.R. Grimmer, A high resolution ^{29}Si NMR study of the hydration of tricalciumsilicate, Cem. Concr. Res. 12 (1982) 597–602.
[25] J. Rottstegge, M. Wilhelm, H.V. Spiess, Solid state NMR investigations on the role of organic admixtures on the hydration of cement pastes, Cem. Concr. Compos. 28 (2006) 417–426.
[26] G. Engelhardt, D. Michel, High-Resolution solid-state NMR of silicates and zeolites, Wiley, Chichester, 1987.
[27] S. Emid, J.H.N. Creyghton, High resolution NMR imaging in solids, Physica 128B (1985) 81–83.
[28] S. Gravina, D.G. Cory, Sensitivity and resolution of constant-time imaging, J. Magn. Reson. B104 (1994) 53–61.
[29] D. Massiot, F. Fayon, M. Capron, I. King, S. Le Calvé, B. Alonso, J.O. Durand, B. Bujoli, Z. Gan, G. Hoatson, Modelling one and two-dimensional solid-state NMR spectra, Magn. Reson. Chem. 40 (2002) 70–76.
[30] R. Wang, X.-G. Li, P.-M. Wang, Influence of polymer on cement hydration in SBR-modified cement pastes, Cem. Concr. Res. 36 (2006) 1744–1751.
[31] M. Wilhelm, M. Neidhöfer, S. Spiegel, H.W. Spiess, A collection of solid-state ^{13}C CP/MAS NMR spectra of common polymers, Macromol. Chem. Phys. 200 (1999) 2205–2207.
[32] T. Terao, S. Maeda, A. Saika, High-resolution solid-state carbon-13 NMR of poly (vinyl alcohol): enhancement of tacticity splitting by intramolecular hydrogen bonds, Macromolecules 16 (1983) 1535–1538.
[33] A. Comotti, R. Simonutti, P. Sozzani, Hydrated calcium silicate and poly(vinyl alcohol): nuclear spin propagation across heterogeneous interfaces, Chem. Mater. 8 (1996) 2341–2348.
[34] D.A. Torchia, J. Magn. Reson. 30 (1978) 613–616.
[35] A. Comotti, R. Simonutti, P. Sozzani, Morphology of the poly(vinyl alcohol)–poly(vinyl acetate) copolymer in macrodefect-free composites: a ^{13}C magic-angle-spinning nuclear magnetic resonance and ^{1}H spin-diffusion study, J. Mater. Sci. 32 (1997) 4237–4245.
[36] S.K. Mallapragada, N.A. Peppas, P. Colombo, Crystal dissolution-controlled release systems: II. Metronidazole release from semicrystalline poly(vinyl alcohol) systems, J. Biomed. Mater. Res. 36 (1997) 125–130.
[37] S.K. Mallapragada, N.A. Peppas, Dissolution mechanism of semicrystalline PVA in water, J. Polym. Sci. Polym. Phys. 34 (1996) 1339–1346.
[38] R.M. Hodge, G.H. Edward, G.P. Simon, Water absorption and states of water in semicrystalline poly(vinyl alcohol) films, Polymer 37 (1996) 1371.